7.3 Pointing servo system

7.3.1 Fundamentals of servo systems

The basis of a telescope's closed-loop servo system consists of continuously comparing the actual pointing direction to the desired pointing and "feeding back" any difference to the drive system for correction. This process is represented graphically in Fig. 7.5.

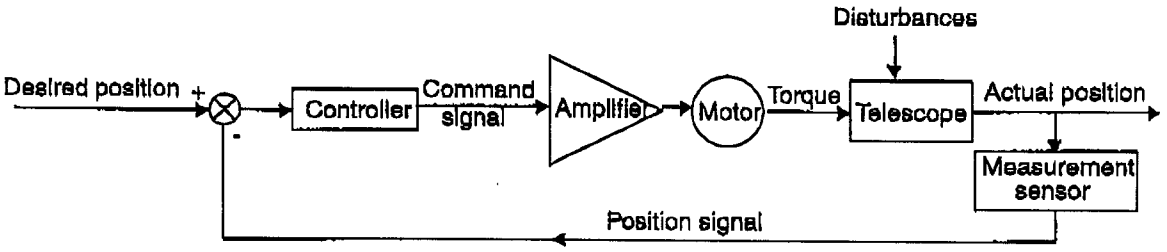

Fig. 7.5. Basic functional block diagram of the pointing servo system. The actual position is compared to the desired position; then, the corresponding error is fed to the drive system to correct the position.

The main components of the control system are the position sensor (or encoder), the controller, and the drive system chain (amplifier and motor). With the advent of computers, the desired position signal is now produced digitally, and the measurement of the actual position is generally also digital. The low-level-signal part of the control system is thus digital, and a digital-to-analog converter is used to feed the command signals into an amplifier, which, in turn, drives the motors.

The purpose of the "controller" is to supply a command signal based on the error detected. It should be designed to minimize that error as quickly as possible without creating instabilities. In its simplest form, the controller could supply a command signal proportional to the error signal: the greater the error, the greater the command torque, and as long as the error remains, the controller will generate a corrective command. Increasing the controller gain (the proportionality coefficient) will boost the correction signal and reduce the time needed to reach correction. This can be done up to the point where the overshoot becomes too large and the system is unstable. This type of controller is called a "proportional controller." The problem with proportional controllers is that they suffer from steady-state error. Because of friction in the drive chain (in gearboxes, rollers, motor shafts, etc.), the motors cease to act when the error signal is just below the point required to break friction. The telescope will sit there with that error and the corresponding command torque, but will not move. The solution is to introduce an *integrator* term in the control law. With integral action, the controller's output is proportional to the time during which the error is present and will eventually force the

telescope to move. This type of controller is called "proportional-integral" (PI).

Integral action has a destabilizing effect due to the increased phase shift, however, so that a lower gain must be used, resulting in longer response time. The proportional-integral controller is thus more accurate and will correct low-frequency errors well, but will be less responsive at higher frequencies. The remedy is to introduce a *differential* term in the control law so that controller output is proportional to the rate of change in the error. The differential term will permit swift correction of rapid changes in the error signal and thus inhibit overshoots and allow for higher gain. This results in a faster settling time and higher correction bandwidth. Most controllers are of this type, called "proportional-integral-derivative" (PID). The price one pays is higher sensitivity to sensor noise, since the derivative of a fluctuating signal also fluctuates. Most PID controllers are thus equipped with noise filters to minimize extraneous fluctuations.

The general behavior of these three types of controller is well illustrated in Fig. 7.6, which shows their typical response to a step input.

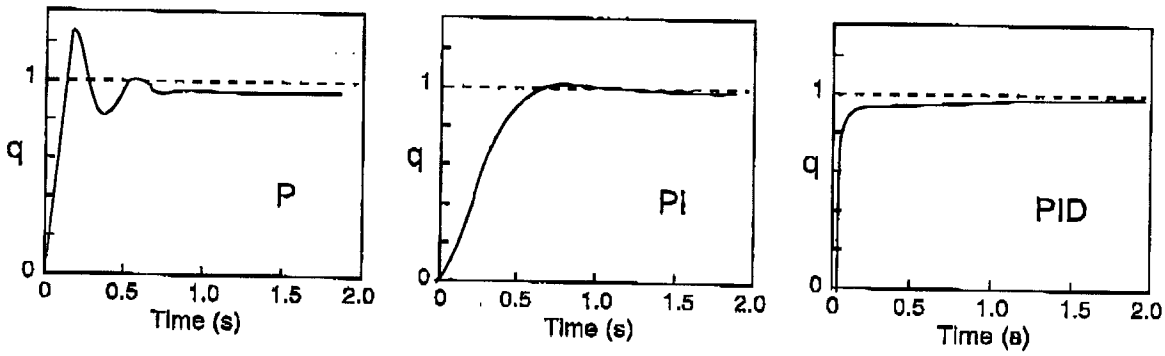

Fig. 7.6. Typical responses of a servo system to a step input. The response (q = outut/input) of a proportional controller is shown on the left. The response time is good but a steady-state error is present and there is some overshoot. Adding an integral term eliminates the steady-state error and reduces the overshoot, but at the expense of a slower settling time (center). Adding a derivative to form a PID controller leads to a system with no steady-state error, no overshoot, and rapid response (right).

The control law of a PID controller is of the form

$$u = K_p e + K_i \int e\, dt + K_d \frac{de}{dt}, \tag{7.14}$$

where u is the corrective command signal, e is the error signal, and K_p, K_i, and K_d are the proportional, integral, and derivative gains, respectively.

The optimal values for these control-law coefficients are obtained by combining a mathematical model of the system being controlled with the control law, then performing an analysis of the control system. This mathematical representation leads to a set of simultaneous differential equations which are

linear if the system is linear. The most popular approach for solving these differential equations is by the use of the Laplace transform, which transforms derivatives and integrals into algebraic expressions. Various techniques are then used to determine the stability domains, the response to command and disturbances, and the optimal control law. A description of these techniques can be found in standard textbooks such as those listed at the end of this chapter.

7.3.2 Telescope control system implementation

Control law for space telescopes

The block diagram of a typical space telescope control system is shown in Fig. 7.7 [12]. The three-axis torque commands are developed via a digital PID controller in series with low-pass filters for attenuation of the structure's flexible modes. Gyroscopes and star trackers serve as sensors for attitude determination and their data are optimally combined with the guiding system information via a Kalman filter to minimize the effects of sensing noise and drift (see discussion later in this subsection).

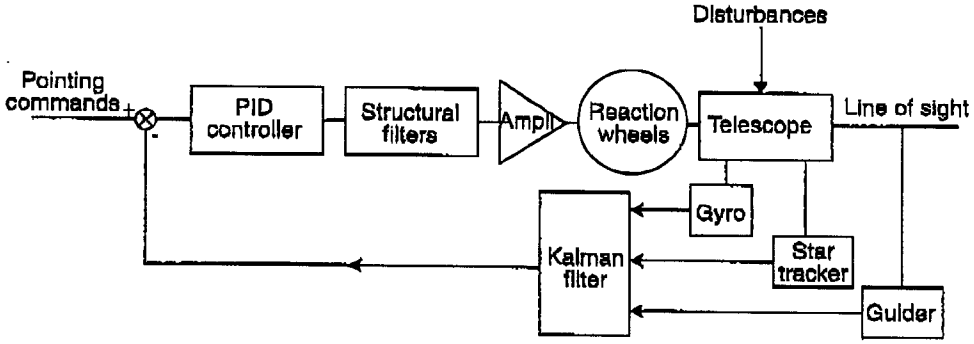

Fig. 7.7. Block diagram of a space telescope control system.

The tuning of the controller is fairly straightforward. The telescope is first modeled as a rigid body and the PID gains are set to produce adequate gain and phase margins[1] (e.g., 12 dB and 30°, respectively). The flexible body dynamics are then added to the model, and the cutoff frequencies and orders of the structural filter are determined such that the closed-loop system is stable (e.g., with a 10 dB margin).

Ground-based telescopes

The control systems of ground-based telescopes differ somewhat from those of space telescopes because of the different nature of disturbances encountered. The space environment is benign and friction effects are almost nonexistent

[1] See glossary.

due to the absence of gravity. On the ground, control systems must be more aggressive to combat larger torques and react better to nonlinearities (see Section 7.3.3). The solution consists of emphasizing the control of velocity and is generally accomplished by using two separate feedback loops as shown in Fig. 7.8: a velocity loop and a position loop.

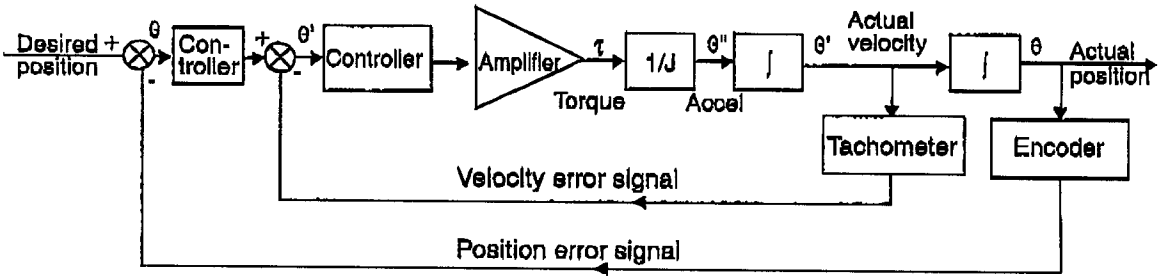

Fig. 7.8. Position loop with nested velocity loop. The velocity signal is either obtained with a dedicated tachometer or derived from the position encoder.

The velocity loop tightly controls the dynamics of the telescope structure and rejects disturbances such as wind and friction. The loop is usually implemented with a PI controller to maximize responsiveness, combined with a filter to avoid exciting resonance frequencies in the telescope structure. In practice, it is only possible to extend the bandwidth up to about 60% of the lowest locked rotor frequency of each telescope axis. A typical velocity-loop frequency response is shown in Fig. 7.9.

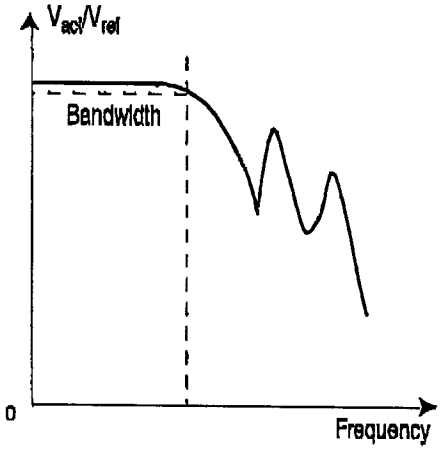

Fig. 7.9. Notional frequency response of the velocity loop for a ground telescope. The loop acts as a low-pass filter with a bandwidth of about 60% of the first locked rotor frequency.

With velocity control solved, the position loop's task is reduced to maintaining zero tracking error and to handling large changes in the desired position. During tracking (small excursions), a PI controller is used to maximize responsiveness. Large steps in position commands (large offset requests, repointing) are handled with a special algorithm.

The respective roles of the velocity and position loops can then be summarized as follows: the velocity loop takes care of the *dynamics* of the telescope structure, whereas the position loop takes care of pointing *accuracy*.

Guiding loop

The control systems discussed above are inherently limited in pointing accuracy by the *absolute* accuracy of the encoders or attitude sensors. Not only may their angular resolution not be high enough to track celestial objects, but a number of effects of optical (distortion), mechanical (optical/boresight/encoder alignment), thermal (alignment changes), and astronomical origin (atmospheric refraction) introduce additional errors. Although some of these effects can be calibrated out, residual errors are generally still significant. Fortunately, the sky itself can provide a final check on the pointing position by the observation of a star inside the telescope's field but outside the science field. Until the 1960s, this process, called "guiding," was carried out by the observers themselves, who made corrections manually. Guiding is now done automatically using an image centroiding device called a "guider." Details on how the corrective signal is obtained will be given in Section 7.5.5. This error signal can be used in two ways. It can either be fed to the position loop as additional position-error information or form an additional correction layer totally independent of the main control servo system (Fig. 7.10).

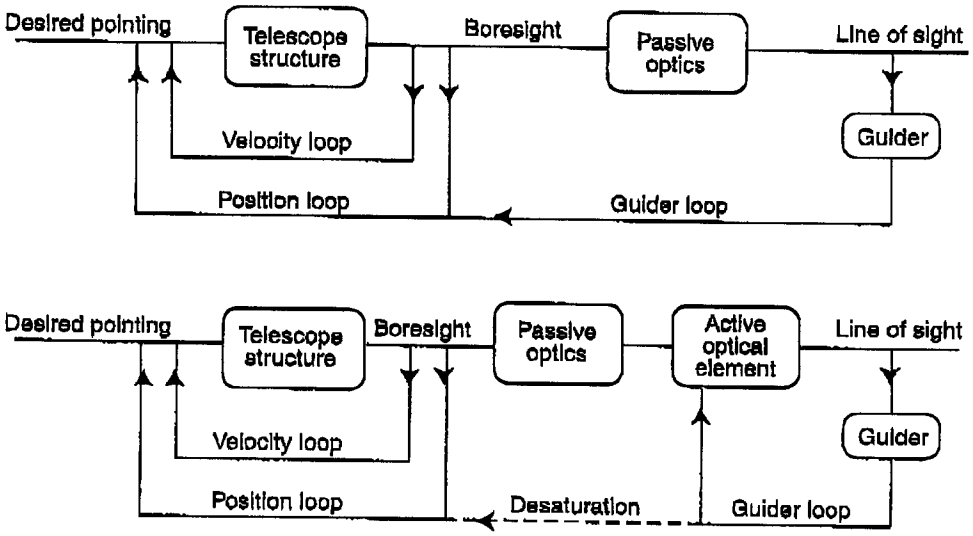

Fig. 7.10. The two schemes for using the guiding system error signal. On top, the guiding error signal is blended into the position error signal of the main control loop. At bottom, the guiding error signal is used to drive an active optical element which corrects the line of sight while leaving the telescope structure pointing unchanged. When the active optics correction becomes too large and the optical angular correction reaches physical or optical quality limits, the active optics loop is "desaturated" by feeding an error signal to the main pointing system.

7.3.3 Disturbance rejection

"Disturbances" are those undesirable forces and torques acting on the telescope system that perturb its operation because they are not under the direct influence of the controller the way the drive motor torque is. They include (1) external torques such as those due to wind or the space environment and (2) internally generated effects such as friction in bearings, motor ripple, and mechanism motion in the telescope and instruments. The origin and analysis of such disturbances will be investigated in detail in Sections 7.6 and 7.7. From the point of view of the control system, disturbances fall into two categories: linear and nonlinear.

Linear disturbances

Linear disturbances are those that create a parasitic force or torque such that the system is still governed by linear differential equations with constant coefficients (such as those of Section 7.2.1). The problem with nonlinear differential equations is that they are not solvable in closed form. Some nonlinear disturbances can still be treated in the traditional fashion, however, because their behavior is near-linear; that is, they are essentially linear over a small range of input values. This is the case, for example, for motor ripple and wind gusts. To minimize sensitivity to such linear disturbances, one must

- increase the bandwidth and servo gains of the telescope control system to cover the frequency spectrum of the disturbance with sufficient rejection power;
- decrease the magnitude of the disturbance by protecting the telescope (e.g., placing it in an enclosure and behind a windscreen to reduce wind effects), by reducing the cross sections of telescope members, or by passive or active isolation; or
- add a special control loop to actively compensate for the effect of the disturbance.

The first approach only works if the telescope can be stiffened. The second approach will be examined later in this chapter and in the chapters on enclosures and site selection.

The third approach has not yet been implemented, but there have been proposals. Since wind is, by far, the main disturbance on ground-based telescopes, a "wind feed-forward loop" was proposed for the control system of the VLT. Wind speed was to have been measured with a fast-response sensor immediately upstream of the telescope and a correction torque injected into the servo system at the proper time to counteract gusts. It is estimated that if this kind of ad hoc correction loop were adopted, the line-of-sight jitter due to wind could be reduced in the VLT by a factor of 2 [15].

Nonlinear disturbances

Nonlinear disturbances are more problematic in the sense that they cannot generally be eliminated by the control system. This is the case with friction. In Section 7.2.1, we assumed that damping was linear with the angular velocity. In reality, this is only true when velocity is not close to zero. At near-zero velocity, friction creates abrupt changes in velocity, a phenomenon referred to as "stick-slip" (Chapter 6), resulting in cyclic position errors, as shown schematically in Fig. 7.14. For sophisticated analysis, this effect can be represented mathematically using the "Dahl model" [16].

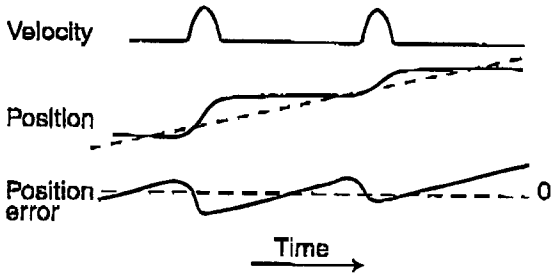

Fig. 7.14. Stick-slip near zero velocity creates abrupt changes in velocity (top) that result in cyclic position error (bottom).

To minimize stiction or any other nonlinear discontinuous torque source, the control system must have a high enough bandwidth for the servo to detect a rapid change in the mount response and quickly increase or decrease torque to overcome it. If the telescope relies only on a low bandwidth position loop (and all position loops wrapped around the largest system inertias are low-bandwidth), then the motion at around zero velocity is going to be jittery. On the other hand, if a high-bandwidth velocity loop is wrapped around the motor with tachometer feedback, this loop can detect an instantaneous change in speed resulting from a step in friction and quickly respond to correct the problem. If the bandwidth of the velocity loop is so high that the position loop is insensitive to it, then the result in position control will be an almost flawless transition through the zero-velocity regime. This type of control incorporating a separate velocity loop is essential for combating nonlinearities in ground telescopes.

In addition to solid friction due to bearings, gears, seals, motor brush drag, etc., several other nonlinearities may affect smooth operation of the control system. They include

- gear backlash,
- nonlinear spring rates of bearings, gears, and gearboxes,
- sudden torque changes in cable wraps other than those due to solid friction,
- quantization of digital commands,
- encoder and tachometer quantization,

- time delays, usually associated with sample-and-hold data,
- operational discontinuities such as step commands.

Methods to reduce the effect of nonlinearities include

- avoiding solid friction altogether by using hydrostatic bearings and minimizing the impact of other sources of nonlinearities by design,
- maximizing the inertia/friction ratio,
- using a separate drive to move cable wraps,
- avoiding driving the servo gains higher than needed, especially the integrating gain in the position loop (the drawback being an increase in wind sensitivity),
- avoiding zero velocity by incorporating a continuous mechanical motion stage in the drive with no effect on pointing, or by "biasing" the velocity of the drive system to avoid zero velocity altogether, as can be done with reaction wheels in space telescopes (see Section 7.4.2),
- "dithering," which consists of feeding a constant sine wave torque command to keep the drive system restless (with the drawback of increased wear).

When the nonlinear behavior is repeatable and predictable and can be characterized, its effects can be countered by introducing a command at the right time to create a motion of the telescope exactly opposite to that of the nonlinear effect. This is what was done on the Hubble Space Telescope to eliminate the jerk created by friction when the reaction wheels go through zero velocity. The time of "zero crossing" is predicted by monitoring the wheel speed as a function of time and, at the predicted time, a pulse command in the opposite direction is introduced by the pointing-control system.

As telescopes become larger, their sensitivity to disturbance increases because of sheer size, so that the value of the above solutions diminishes. Fortunately, there is a way out which consists of adding a new control layer to act directly on the optical path instead of on the structure supporting the optical elements. With this, we enter the realm of active and adaptive optics, which will the subject of Chapter 8.

7.4 Attitude actuators

7.4.1 Drives for ground-based telescopes

Until the 1970s, most ground-based telescopes used a worm gear system because its high gear ratio and excellent intrinsic accuracy permitted open-loop tracking using a constant-speed motor. The worm gear offers a large speed ratio in a single pair (e.g., 1/720), resulting in a very stiff drive [17]. Moreover,

When the wheel rotation has to reverse, there will be an undesirable pulse on the telescope as the wheel speed goes through zero and torque is suddenly increased to overcome friction. This effect can be compensated by introducing an opposite torque at the exact time the wheel speed passes through zero, as was done on HST (see Chapter 6). Another approach is to simply bias the wheel speed so that the rotation sense never does reverse. For example, instead of operating within a range of −1000 rpm to +1000 rpm, one can center wheel speed on +1100 rpm and operate between 100 and 2100 rpm.

Momentum dumping

Space telescopes have to combat an external torque due to imbalanced solar radiation pressure (and residual atmosphere in near-Earth orbit) which, although small, does accumulate to significant values after several hours. This torque is continuously counterbalanced by the reaction wheels, but their spin speed will progressively build up, and control of the spacecraft will be lost when the wheel speeds reach their maximum values. Accumulated momentum must be eliminated before this happens. This is generally accomplished by use of a mass ejection device such as a gas thruster or magnetic torquers for near-Earth orbits.

7.5 Attitude sensors and guiding system

Pointing a telescope at a given target requires the ability to determine the absolute direction of the optical axis. For ground-based telescopes, the position of each axis is measured by position encoders mounted on each of the moving axes. For space telescopes, the main attitude sensors are generally gyroscopes, the drifts of which are corrected by star trackers.

7.5.1 Position encoders

In early telescopes, the polar axis and declination axis shaft angles were determined visually using "hour and declination circles." These were simply large circles mounted on each axis, with scaling marks every 10 arcminutes or so. These circles were later replaced by a pair of transmitting synchros mounted on the drive systems, with repeater synchros at the console. Today's telescopes employ position encoders (more commonly called simply "encoders"), which are the modern equivalents of hour circles and nearly always of the optical type. Optical encoders consist of a series of reference marks on some sort of support and a counting head which reads these marks. The support can be a tape wrapped around a cylindrical surface coaxial with the telescope axis or a disk mounted perpendicular to the axis. The marks are read by a noncontacting, self-adjusting optical head, which means no wear and low maintenance. The reference marks have a linear accuracy which can be as good as 3 μm for

linear tapes and 1 μm when a very stiff special glass or quartz substrate is used.

Encoders fall into two categories: incremental and absolute. An absolute counting encoder "knows" the absolute position upon being turned on, whereas an incremental encoder does not. Incremental encoders simply supply a differential position measurement. However, if referenced to an absolute position, an incremental encoder will also provide an absolute measurement (potentially with even higher accuracy than that of an intrinsic absolute encoder), although miscounts can happen due to dust, grease or vibration.

An example of an incremental optical tape encoder is shown on the left in Fig. 7.22. A grating on a tape is imaged through a set of four gratings, each being phase-shifted from the others by one-quarter of the grating period. As the tape moves with respect to the reading head, the light-dark modulation produced by each of the scanning gratings is read electronically. The four signals are then combined to produce an incremental measure of the tape's displacement. For absolute encoding, a number of tracks are added to allow unique determination of the position by the use of some encoding technique. The principle is shown on the right in Fig. 7.22 for a rotary encoder.

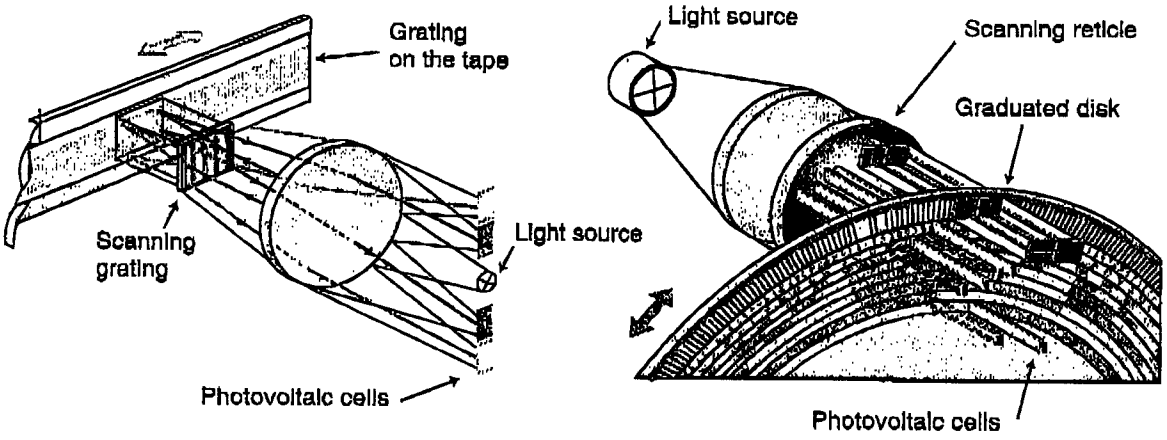

Fig. 7.22. Examples of an incremental optical tape encoder (left) and of an absolute disk encoder (right). In these implementations, the tape is metallic and is measured by reflected light, whereas the absolute encoder uses a glass disk and transmitted light. (Courtesy of Heidenhain Corporation.)

Absolute encoders are generally mounted directly on a large journal and used for absolute pointing determination. They have an intrinsic absolute accuracy of about 1″. Incremental encoders can have a higher angular resolution (e.g., 0.1″) and are typically used for tracking. They are sometimes mounted on a gear or friction system for increased magnification. Tape encoders should be mounted on as large a lever arm as possible to maximize resolution [20]. In the case of the VLT, which uses such encoders, tapes have grid spacings of 40 μm and a diameter of 1.6 m for the altitude axis and 7 m for the azimuth axis.

7.5.2 Tachometers

Tachometers are used to supply velocity information to the velocity loops of ground-based telescopes. They should be mounted close to the drive in order to achieve dynamic stability. It is important to understand that the performance of the control loop at medium to high frequency (i.e., the domain where the position loop is insufficient) depends entirely on, in fact mimics, the tachometer signal. The choice of origin, processing, and placement of the tachometer system is consequently critical to the performance of the whole system.

A traditional solution consists of using conventional brushed DC tachometer generators on a roller mounted on the journal used in driving the telescope axes. The roller mechanism should be totally separate from that of the drive, to avoid corrupting the velocity information by torsion stress, and it should have a flexible mount in order to follow any runout in the driven journal. But as a result, this flexible mount will allow small rotations of the whole tachometer assembly at rotation reversals. This means that the tachometer will not be able to measure correctly through the zero-speed range of the telescope, that it will have backlash there, and that this will result in the telescope oscillating across zero speed.

In geared systems (not in direct drives), an alternative is to mount the tachometer on the drive motor shaft, but care must be taken to prevent the tachometer from being sensitive to commutation spikes and mechanical deformation induced by the motor. Furthermore, this solution would close the loop on motor speed, not telescope speed, thus allowing the transmission inaccuracies to be passed along to the optical system.

To avoid the problems associated with rollers, the tachometer can be of the "direct drive" type, working in reverse mode to that of a direct drive motor. This solution is exempt from nonlinearities, but a direct tachometer for a telescope must be endowed with enormous sensitivity to magnetic field gradients in order to produce a meaningful signal at speeds well below 1 turn/day. This sensitivity is feasible but also means that such a direct tachometer would be sensitive to magnetic flux variations in or near the telescope's steel structure. Such direct, analog tachometers were originally implemented on the VLTs, but had to be abandoned for this reason.

All systems described so far involve a brushed, mechanically or electronically commutated DC generator which produces an analog voltage proportional to telescope rotation speed. Apart from the intrinsic limitations in the device itself, the analog signal is awkward because of the extremely wide speed range required for telescope pointing and tracking: during tracking, the tachometer signal must retain a good signal-to-noise ratio although the signal is at the submillivolt level. This is clearly impractical. Recent designs have therefore resorted to obtaining tachometric feedback by processing the digital signal of the main telescope encoders [21].

Using the encoder data is an ideal solution from mechanical and rational viewpoints. All ground-based telescopes must have quality encoder systems, intrinsically free from backlash and stick-slip, and with subarcsecond accuracy. The needed signal is therefore readily available. This apparently simple solution faces two main problems however:

- Encoders read position, so the speed signal must be obtained by differentiating the encoder readings at two consecutive readouts. This must be done rapidly enough to avoid compromising the dynamic performance of the system. Usually, the raw encoder data needs extensive processing, so there may be a computing-time problem.
- Although the encoder error is always lower than the telescope pointing accuracy, typically less than $0.1''$ in large telescopes, this error may have a very high spatial frequency. Consequently, the "ghost" speed ripple caused by encoder error, amplified by the differentiation process, may impair the performance of the speed loop.

These problems require careful design and programming, but this new "digital tachometer" approach is in line with the evolution of servo technology in industrial applications, from which analog tachometers disappeared in the early 1990s.

7.5.3 Gyroscopes

A gyroscope consists of a rapidly spinning flywheel used to sense and measure changes in the orientation of the spin axis (the name is often abbreviated to "gyro"). The most common type of gyroscope for spacecraft attitude sensing is the "single-degree-of-freedom rate gyro." Single degree of freedom refers to the fact that the flywheel is mounted on a single gimbal and only the corresponding axis is sensed. Three gyros with different orientations are thus needed to measure all three angles of attitude. Rate gyros are so called because they measure the angular rate of change in the direction of the spin axis (by opposition to rate integrating gyros, which provide the total spacecraft rotation from an inertial reference).

A single-degree-of-freedom rate gyro is represented schematically in Fig. 7.23. The gimbal is restrained by viscous damping and a restoring spring, and the rotation of the output axis is proportional to the spacecraft's angular rate about the input axis. In actual high-accuracy gyros such as those used on space telescopes, the spin axis is supported by gas bearings and the output axis rotation is balanced by an electromagnetic torque. The applied torque is the measure of the angular rate.

The HST gyros, despite their technology dating from the 1970s, are still state of the art. They have an angular resolution of 0.25 mas and drift at the rate of 1 mas/s [22]. They need to be corrected every few seconds with absolute positional data supplied by star trackers or fine guiding systems.

of mechanisms in the instruments (e.g., filter wheels), torque ripple in the drive motors, and friction in the telescope axes and in the cable wraps. Mechanism motion is generally insignificant because of the large moment of inertia of the telescope itself, whereas torque ripple and friction sources can usually be dealt with by proper design of the control system, as discussed in Sections 7.4.1 and 7.5.

By far the largest source of disturbance in ground-based telescopes is wind. Its effects are particularly detrimental because its power spectrum contains considerable energy at low frequencies (0.1 to 1 Hz), which are relatively close to resonance frequencies in the structure and active mirror systems.

Most astronomical sites are in isolated locations at high altitude and, as a result, are quite windy. To maintain observing efficiency, observatories are usually designed such that observation remains possible for 95% of the "clear sky" time. This results in a requirement to operate in fairly high wind conditions (e.g., up to 20 m/s at the Mauna Kea observatories).

7.6.1 Effects of wind: Generalities

Wind effects on any structure are of two sorts: static and dynamic. The static effect is simply due to the pressure created by a constant wind on surfaces impinged upon. Dynamic effects stem either from the turbulence created by an obstructing surface in a flow with constant speed or from turbulence in the incoming flow itself.

Wind static effects

Wind load on any structure is given by

$$F = C_D \rho \frac{V^2}{2} A, \tag{7.21}$$

where C_D is the drag coefficient, ρ is the density of air, v is the velocity of air, and A is the cross-sectional area normal to wind direction. The drag coefficient depends on the geometry of the body, the turbulent state of the incident wind, and the wind velocity. Assuming that the incident flow is laminar, the drag coefficient can be described as a function of geometry and of the Reynolds number.[3] The drag coefficient for flat plates is equal to 2, whereas for cylindrical shapes, it varies between 0.4 and 1.2, depending on the Reynolds number [29].

[3]The Reynolds number is given by $\mathcal{R} = VL/\nu$, where L is the characteristic dimension of the object normal to the flow, V is the flow velocity, and ν is the kinematic viscosity of the fluid ($\nu = \mu/\rho$, where μ is the dynamic velocity). At Mauna Kea (4200 m altitude, -10 °C temperature), $\rho = 0.82$ kg/m^3, and $\nu = 2.0 \cdot 10^{-5}$ m^2/s.

Dynamic wind effects: Vortex shedding

In addition to the direct drag force examined above, airflow around individual members can generate forces normal to the wind direction due to "vortex shedding" (also called Von Karman vortices). Vortex shedding can excite natural resonances in the member and result in large-amplitude oscillations. Karman vortices are shed at the characteristic frequency, f, given by

$$f = \frac{\mathcal{S}V}{L}, \tag{7.22}$$

where V is the wind speed, L is the characteristic transverse dimension of the element, and $\mathcal{S}$ is a dimensionless quantity called the Strouhal number, which depends on the Reynolds number but is typically around 0.2. Hence, the vortex shedding frequency for cylinders is approximately given by

$$f = \frac{0.2V}{L}. \tag{7.23}$$

Dynamic wind effects: Wind gustiness

The turbulence content in a wind flow is characterized by the power spectral density (PSD) of the wind speed. Two models are commonly used for wind speed PSD near the ground: the Von Karman spectrum and the empirical Davenport model. The Von Karman spectrum is defined as

$$S_V(\nu) = \frac{4\,I^2\,V^2 L}{[1 + 70.8(fL/V)^2]^{\frac{5}{6}}}, \tag{7.24}$$

where ν is the frequency, I is the turbulence intensity in percent, V is the mean speed in m/s, L is the outer scale of turbulence in meters, and S_V is the PSD in $(\mathrm{m/s})^2/\mathrm{Hz}$. In open air, I is about 15% and L is on the order of 80 m. Inside the telescope enclosure or downstream from a porous wind screen, the incoming wind vortices are broken down into smaller ones, with size driven by the dimension of the obstruction (dome slit, louvers, etc.), and L is set by that dimension. For a telescope enclosure with a 10 m wide slit for example, L has been found to be 3.2 m. A comparison of the power spectrum inside and outside an enclosure is shown in Fig. 7.27, left.

The other frequently used power spectrum density model is the Davenport formula which was derived empirically [30, 31] as

$$S_V(z,\nu) = \frac{4.0\,k\,x^2\,V^2}{\nu\,(1+x^2)^{4/3}} \quad \text{with} \quad x = \frac{1200\,\nu}{V_{10}}, \tag{7.25}$$

where $S(z,\nu)$ is the PSD at height z in $(\mathrm{m/s})^2/\mathrm{Hz}$, ν is the frequency in Hertz, V is the mean wind velocity at height z, V_{10} is the mean wind velocity at a height of 10 meters in m/s, and k is a roughness coefficient, which is about 0.08 for open terrain. As shown on the right in Fig. 7.27, this formula has proved to match data obtained at typical astronomical sites.

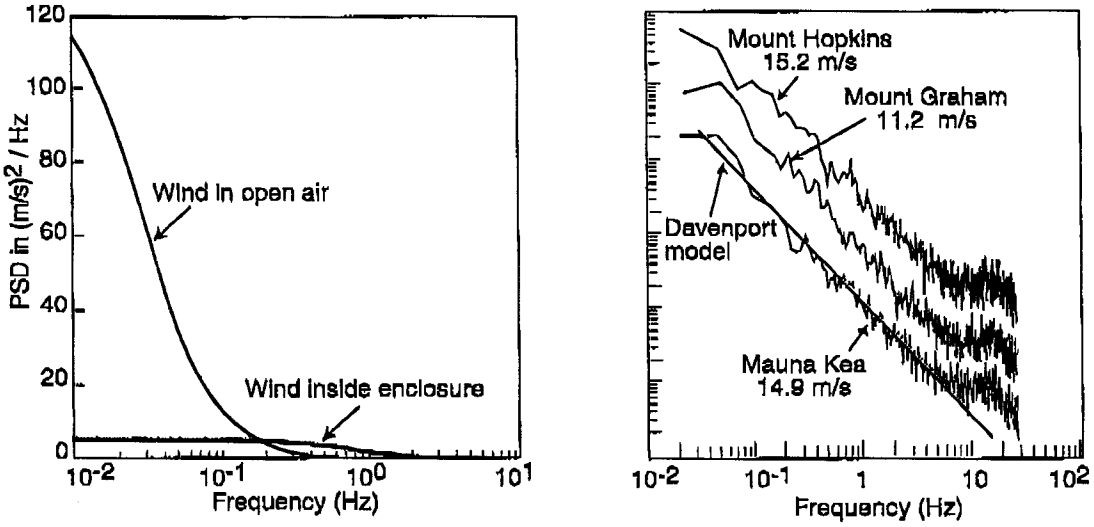

Fig. 7.27. At left, power-spectrum density inside a telescope enclosure compared to that of the outside wind. Although much reduced in amplitude, the wind inside the enclosure might still be damaging to image quality because its power spectrum is shifted to higher frequencies which are more prone to excite the telescope structure or active mirror systems. At right, power-spectrum density of the wind at three representative astronomical sites. The power spectra have been displaced vertically for clarity, but have the same magnitude. The straight line is the Davenport model, which is valid for undisturbed flow in open terrain. The higher amount of energy between 8 and 30 Hz compared to the Davenport model is thought to be an artifact of the measurement.

When wind acts on a large structure such as a telescope, one must take into account the partial decorrellation of the wind speed over the telescope area facing the wind. This is done by applying an aerodynamic attenuation factor, χ_a, which is given by

$$\chi_a^2(\nu) = \frac{1}{1 + (2\nu\sqrt{A}/V)^{\frac{4}{3}}}, \tag{7.26}$$

where A is the characteristic area facing the wind. For very large structures, the attenuation factor is quite significant, so that the influence of wind turbulence is negligible.

7.6.2 Effects of wind on telescope structure

Static and dynamic wind loads

Static wind load can be readily estimated from equation 7.21. As for dynamic wind load, the PSD of the wind torque around a given axis, S_τ, is given by

$$S_\tau(\nu) = \tau^2 S_V(\nu) \chi_a^2(\nu), \tag{7.27}$$

where τ is the static wind torque around that axis, $S_V(\nu)$ is the wind speed power spectrum density from equation 7.24 or 7.25, and $\chi_a(\nu)$ is the aerody-

namic attenuation given by equation 7.26. As an example, Fig. 7.28 shows the PSD of wind torque on the altitude axis of the VLT. Multiplying this PSD by the square of the control system's rejection sensitivity supplies the PSD of angular rotation around that axis, and integrating this over frequency gives the rms squared of the pointing error [6].

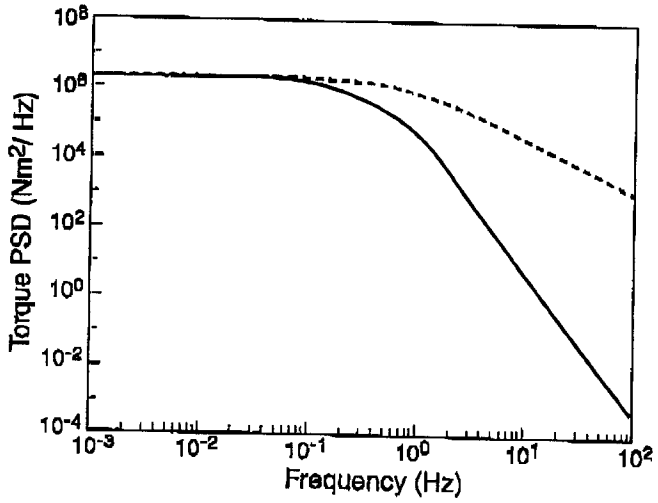

Fig. 7.28. Predicted PSD of wind torque on the altitude axis of the VLT. The dashed line represents the torque PSD without aerodynamic attenuation, and the solid line represents it with that factor taken into account. The plot shows a clear decrease of disturbance at frequencies higher than 1 Hz. The aerodynamic factor reduces disturbance even more.

Vortex shedding

The dynamic effects of vortex shedding on structural members can be estimated from equation 7.23. For cylindrical beams, the characteristic length is simply the diameter of the beam. In a telescope tube, the typical characteristic length (L) of the structural elements varies from centimeters to meters. Hence, vortex shedding frequencies for 10–20 m/s winds will typically be in the range of 1 to 100 Hz. This is also the range of the natural resonance of these elements, so that a careful check of this problem must be made to avoid undue resonances. The transversal force is given by

$$F = C_L \frac{\rho V^2}{2} A \sin(2\pi f t)\,, \tag{7.28}$$

where V is the wind speed, f is the vortex shedding frequency, and C_L is the lift coefficient, which varies from 0.8 for a Reynolds number of $\mathcal{R} = 10^4$ to 0.4 for $\mathcal{R} \geq 10^6$. Compared with equation 7.21, it can be seen that the oscillatory forces are on the same order as the static wind forces.

7.6.3 Effect of wind on primary mirror

A rough order of magnitude of the wind load on the mirror can be obtained from formula 7.21, where $C_D \simeq 1$ for a flat, circular disk and where V is the wind velocity in the dome at the level of the primary mirror. Inside a dome, the wind velocity is about an order of magnitude lower than that of the wind outside. As for the characteristic period of the wind force, it can be roughly estimated from the time it takes a wind gust to pass over the mirror. With a wind velocity of around 2 m/s at the level of the mirror, the main effect should be at a frequency of V/D, or about 0.2 Hz for a 10-meter telescope.

More precise data must be obtained from flow modeling or *in situ* measurements in order to take into account the attenuation by the dome and the scale of turbulence generated by the dome slit. Such measurements were done for the VLT using a 3.5-meter dummy mirror placed in the NTT dome (Fig. 7.29).

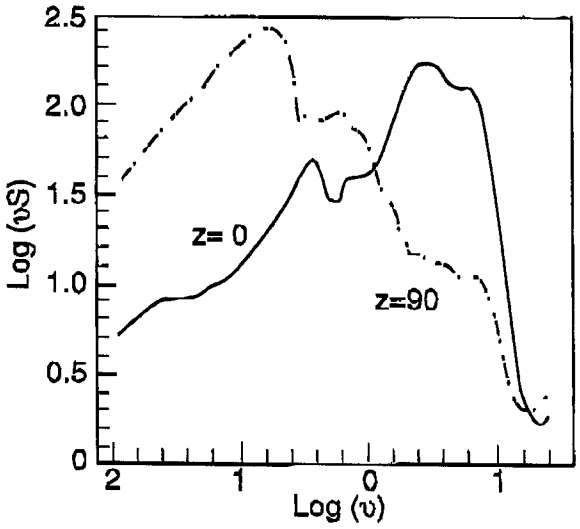

Fig. 7.29. Wind pressure power spectrum on a 3.5 m test mirror inside the NTT dome; mirror pointing to zenith (z=0) and at the horizon (z=90). The power spectrum depends strongly on the inclination of the mirror: the energy is shifted to higher frequencies when pointing to the zenith.

7.6.4 Effect of wind on telescope pier

Under the action of wind on the observatory building, the foundation soils deform and cause tilting of the telescope pier, thus affecting pointing performance during observations (Fig. 7.30). The telescope enclosure presents a very large projected area normal to the direction of the wind, resulting in wind forces in the 10^5–10^6 N range for an enclosure 30 meters in diameter. The associated overturning moment deforms the foundation soil and propagates to the telescope pier, causing image motion in the telescope. The effect

can be estimated very roughly by assuming that the foundation soil behaves elastically [32, 33], but it is best determined by representing the soil as an elasto-plastic semi-infinite solid supporting the enclosure and pier foundation, then solving the problem by finite element computer analysis. Measures to reduce this effect are discussed in Chapter 11, Section 11.7.

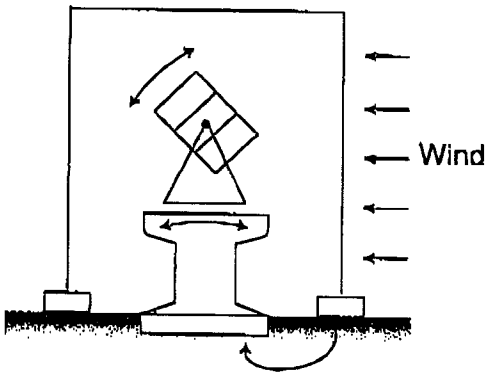

Fig. 7.30. Wind acting on the observatory building creates vibrations which are transmitted to the telescope via the soil and the pier foundations.

7.7 Disturbances in space

A space-borne telescope must contend with a variety of disturbances that potentially degrade both line-of-sight and imaging performance. These may be loosely classified as external disturbances and internal disturbances. External disturbances are the result of interaction with the space environment, and include gravity gradient torque, aerodynamic torque, solar pressure (which generally produces both a force and a torque disturbance), and magnetic torque. Internal disturbances arise from mechanisms aboard the spacecraft such as momentum wheels, thrusters, gyroscopes, filter wheels, and tape recorders, or from the release of strain energy at structural interfaces (joints, latches, hinges) during "thermal snap" events.

External disturbances will not normally degrade either the line-of-sight or the imaging performance of a space telescope. These disturbance torques are either constant or periodic with very low frequencies and are thus well within the bandwidth of a practical attitude control system. Such torques act on the spacecraft, but the resulting momentum is absorbed into the reaction wheels rather than into the body.

Internal disturbances are another matter. These are broadband excitations resulting from impulsive phenomena or, in the case of reaction wheel disturbances, high-frequency and sinusoidal (or multitone) in nature. In either case, there will generally be disturbance components with frequencies outside the bandwidth of the attitude control system that will affect the optical perfor-